

Gender classification via functional connectivity

GUO Siye

Student No 1

LIU Chang

Student No 2

WANG Zeyu

Student No 3

ZHANG Qidan

Student No 4

December 7, 2024

Abstract

Contents

1	Introduction	1
1.1	Gender differences in functional connectivity	1
1.2	Gender classification via machine learning	1
2	Materials and methods	2
2.1	Dataset and preprocessing	2
2.1.1	Human Connectome Project (HCP)	2
2.1.2	Data preprocessing	2
2.1.3	Presentation of Dynamic Functional Connectivity Data	3
2.2	SVM model	4
2.2.1	Methods	4
2.2.2	Results and Conclusions	5
2.3	CNN model	5
2.3.1	Methods	5
2.4	Results and Conclusions	6
3	Analysis	8
3.1	Linear discriminant analysis (LDA)	8
3.1.1	Methods	8
3.1.2	Results And Conclusions	8
3.2	Neuroscientific interpretations	10
4	Discussion	10
References		11
A	Supplementary Material	12
A.1	Ablation study for SVM model	12
A.2	Ablation study for CNN model	13
A.3	Analysis for repetitions	16

1 Introduction

1.1 Gender differences in functional connectivity

As certain forms of psychopathology, such as autism and depression, differ in prevalence across gender, understanding gender differences in the neurotypical brain (NEB) may provide insight into risk and protective factors. It has been shown that functional connectivity (FC) features in the default mode network (DMN), frontoparietal and sensorimotor networks contribute most to the prediction of sex. In the default mode network, the right fusiform gyrus and the right ventral medial prefrontal cortex are important contributing regions. These regions have previously been implicated in multiple aspects of social functioning, suggesting that there may be sex differences in social cognition mediated by the DMN. The findings suggest that sex can be reliably predicted using resting-state functional magnetic resonance imaging (rfMRI) data and highlight the importance of controlling for sex variables in brain imaging studies.

These studies suggest that there may be sex differences in brain networks, so our group hopes to use differences in brain networks to classify genders.

1.2 Gender classification via machine learning

There have been many studies that use brain networks, combined with the processing of data using machine learning algorithms or neural network models, to efficiently predict or classify gender. Table 2 shows that some experiments use static functional connectivity to classify genders, and the accuracy can reach up to 93%. And Table 1 shows the results of some experimental methods using dynamic functional connectivity to classify genders.

Based on these previous study, we consider to use both dynamic and static functional connectivity to classify gender.

Model	Result
SVM	across sample AUC: 0.718(± 0.2) within sample AUC: 0.716(± 0.156)
CNN	rsfMRI AUC: 0.8923 tfMRI AUC 0.7683
SVM	avg ACC: 0.687 max ACC: 0.751
PLSR	AUC: 0.93, ACC: 0.85

Table 1: The models and results of previous papers using static functional connectivity (sFC) to predict gender.

Model	Result
CNN and LSTM	AUC: 0.9805, ACC: 0.9305(± 0.0191)
Statistic analysis	Pearson dFC: ACC: 0.7984 Partial sFC: ACC: 0.9005 Pearson sFC: ACC: 0.6839
Random forest	ACC: 0.94

Table 2: The models and results of previous papers using dynamic functional connectivity (dFC) to predict gender.

2 Materials and methods

2.1 Dataset and preprocessing

2.1.1 Human Connectome Project (HCP)

The project use the Human Connectome Project (HCP) datasets. The HCP has mapped the healthy human connectome by collecting and freely sharing neuroimaging and behavioural data from 1,200 normal young adults, aged 22-35, using a protocol that includes structural and functional Magnetic Resonance Imaging (MRI, fMRI), Diffusion Tensor Imaging (dMRI) at 3 Tesla (3T), and behavioural and genetic testing. Using vastly improved methods of data acquisition, analysis and sharing, the HCP has provided the scientific community with data and discoveries that have greatly advanced our understanding of human brain structure, function and connectivity and their relationship to behaviour. It also provides a treasure trove of neuroimaging and behavioural data at an unprecedented level of detail. Currently, the HCP dataset is widely used to conduct research on the functional connectivity of the human brain.

Our experimental data were taken from timeseries data from the HCP dataset, including the data with nodes (which means numbers of different brain regions) 15, 25, and 50, respectively, which from all 1003 subjects who performed four full fMRI runs (for a total of 4800 time points). Each folder in the dataset contains 1003 txt files, each representing each person's brain network structure. For example, in the 100206.txt file under the 3T_HCP1200_MSMAll_d15_ts2 folder, 4800 rows \times 15 columns of data with IDs of 100206 are recorded.

2.1.2 Data preprocessing

We use timeseries data to examine the functional connectivity between different brain regions. By reading a set of parameters and a file containing the ID of the subject, a directory structure is created for each subject, and a functional connection matrix is calculated based on the time series data.

An easy way to estimate the elements of the covariance matrix is to use the sliding window technique. Based on the given number of nodes, window size, step size, and threshold parameters, a sliding window analysis is performed on the time series data for each subject. Subsequently, the window moves on the timeline and a new correlation coefficient is calculated at each point in time. In this way, we can dynamically evaluate the correlation changes between nodes based on time series data. This approach allows us to capture the structural properties of the data over time without the need for fixed global estimates. The sliding-window correlation at time t is defined as follows:

$$\tilde{\rho}_t = \frac{\sum_{s=t}^{t+w-1} y_{1,s} y_{2,s}}{\sum_{s=t}^{t+w-1} y_{1,s}^2 \sum_{s=t}^{t+w-1} y_{2,s}^2}.$$

According to this definition the correlation at time t is based on w future measurements of the time courses. Then, we can get the dynamic functional connectivity with 15, 25 and 50 nodes.

2.1.3 Presentation of Dynamic Functional Connectivity Data

After preprocessing the data, we used heat maps to show the functional connectivity data of different nodes. As for 15-node charts, there are significant differences in functional connectivity data across different regions. By contrast, when the number of nodes increases to 25, these gaps are remarkably narrowed. Further expanding to 50 nodes, the diagrams show nearly consistent colors across different regions, indicating a high degree of similarity in functional connectivity between different brain regions, which means stronger uniformity between different regions.

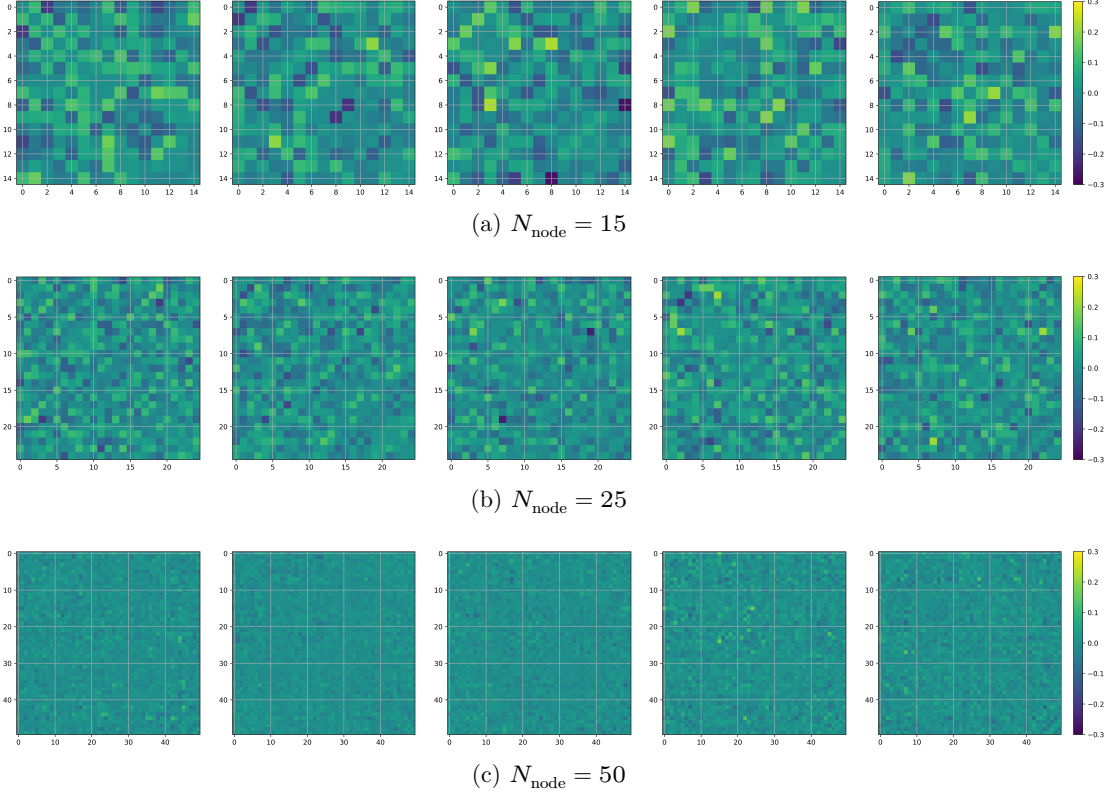


Figure 1: Centered dynamic functional connectivity with $N_{\text{node}} = 15$.

Table 3 shows the maximum, minimum, and average variance of dynamic functional connectivity of different nodes.

N_{node}	min	mean	max
15	5.76e-6	2.80e-5	1.99e-4
25	2.82e-6	1.07e-5	6.07e-5
50	1.63e-8	1.34e-6	4.90e-6

Table 3: Variance of dFC

2.2 SVM model

2.2.1 Methods

SVM is a supervised learning algorithm for classification and regression analysis, the core idea of which is to find an optimal hyperplane in the feature space to maximize the spacing between different classes. So we want to find the most suitable hyperplane to

divide the genders. Since it is hard to determine whether the brain network data is linearly separable before conducting experiments about SVM, we use both the linear SVM and the NuSVM model to train the brain network data respectively.

2.2.2 Results and Conclusions

The experimental results for SVM show that the classification accuracy of the model rises with the increase of nodes of the data. Taking the maximum AUC in different nodes as examples, it is 87.56% for 15-node data, 92.02% for 25-node data, and 97.49% for 50-node data. These numerical results indicate that when the regional features are convergent, the classification accuracy will be correspondingly improved. Additionally, among all tests, the dynamic data of 15 nodes demonstrates the lowest accuracy, which is approximately at 69%. This indicates that both dynamic and static functional connectivity data are linearly separable.

However, when comparing the classification accuracy of dynamic data and static data under the same nodes, the performance of dynamic data is not better than that of static data. This might be attributed to some complex features that dynamic data takes so that it is difficult to extract all of them efficiently using single hyperplane. Therefore, we consider to train brain network data by CNN with ‘multiple hyperplanes’.

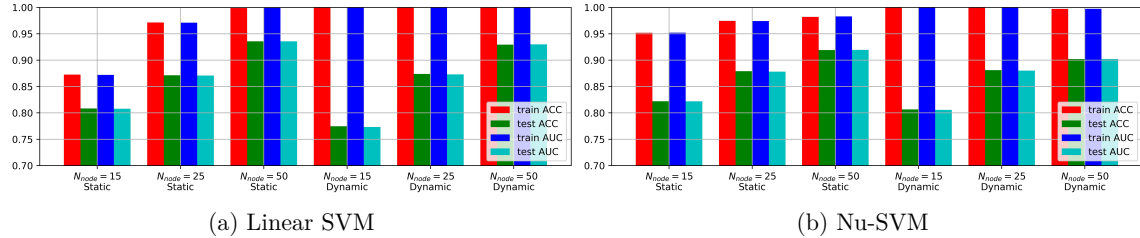


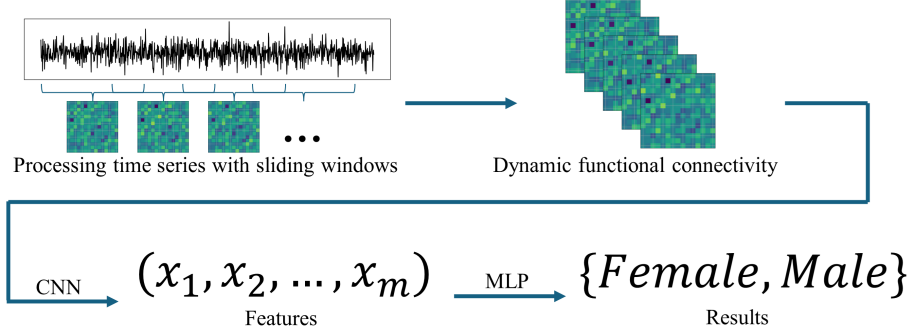
Figure 2: Results of SVM model.

2.3 CNN model

2.3.1 Methods

Convolutional Neural Networks(CNN) is a class of feedforward neural networks with convolutional computation and deep structures. We choose the CNN model because CNN can automatically learn and extract complex features of data through its multi-layer convolution structure, and each layer can be seen as segmenting the data at different levels of abstraction, which is equivalent to using multiple hyperplanes to divide the data. And in the worst-case scenario, where all hyperplanes are the same, the model is linear SVM, and its results should be the same as SVM.

We use m hyperplanes to divide the preprocessed data, extract m feature vectors and correspond to one-to-one, and then use Multilayer Perceptron(MLP) to divide these features into two categories, male and female. The followings are flowchart of our method, where we use a 1-layer 1-dimensional CNN with size equivalent to the input shape, so that it is the same as previous statements.



We split the data into training dataset(80%) and test dataset(20%), and repeat the experiment for 150 times to avoid flukes.

2.4 Results and Conclusions

Figure 3 illustrates the overall results of the data training by CNN. The first 6 columns present the classification results using all frame data, while the last 3 columns describe the results with one frame data that randomly selected. It is remarkable that the classification accuracy is significantly lower when using parts of frame data.

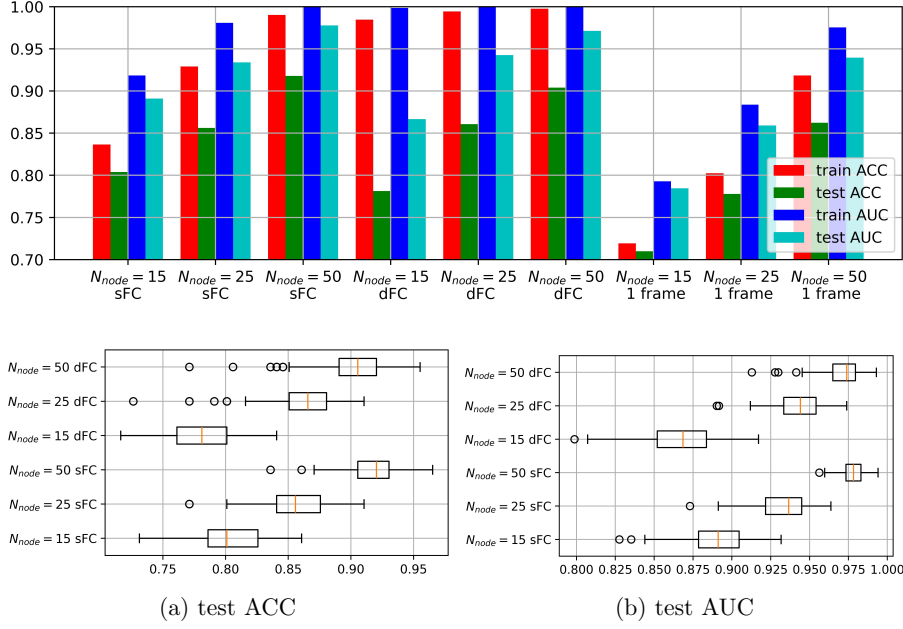


Figure 3: Results of CNN model with dropout = 0.1 and channel = 4.

The appendix A.2 shows detailed accuracy with all the frame data. In general, classification accuracy still grows with the increase of the number of nodes. However, when comparing the classification accuracy from data with the same nodes, we find that the number of output channels, whether to use dropout normalization, and even using different states of brain network data show little difference in the average and highest accuracy. At 15 nodes, the average AUC and maximum AUC are around 87% and 92% respectively. At 25 nodes, these values are around 93% and 97%. At 50 nodes, these values are around 97% and 99%. The differences in above conditions mainly affect the value of the lowest classification accuracy. To be more specific, when the number of output channels increases or the dropout normalization is not used, the lowest value will be slightly higher than that of other conditions. But it keeps almost the same when processing different states of data with controlling other above experimental conditions, which means that the dynamic data does not perform much better than static data although we try to extract more dynamic features.

3 Analysis

3.1 Linear discriminant analysis (LDA)

3.1.1 Methods

To gain a deeper understanding of the data distribution, we processed the brain network data using linear discriminant analysis (LDA), which is used as a statistical method to find the optimal linear combination to maximise between-group variance and minimise within-group variance. Specifically, for a given dataset $\{x_i, y_i\}_{i=1}^N$, the LDA aims to find a vector pair y, c such that the inner product $\langle x_i - c, y \rangle$ minimizes the interclass variance and maximizes the distance between the projected means of the classes.

3.1.2 Results And Conclusions

The following diagrams are distribution plots of both static and dynamic data in different nodes. Firstly, there are overlapping parts in the data distribution of male and female under different nodes, and these regions may represent the common brain network characteristics or functional connectivity patterns of both genders. In addition, with the increase of the number of nodes, the area of overlapping parts becomes smaller, which supports one of the conclusions in chapter 2 that more nodes lead to more accurate results.

At the same time, we also use box plots to show outliers in the sample that are far from the median points. These outliers are present in both dynamic and static brain network data, with the dynamic data exhibiting no fewer outliers than the static data. Such points might have negative impacts on the experimental results, thereby reducing the accuracy of gender classification especially using dynamic brain network data.

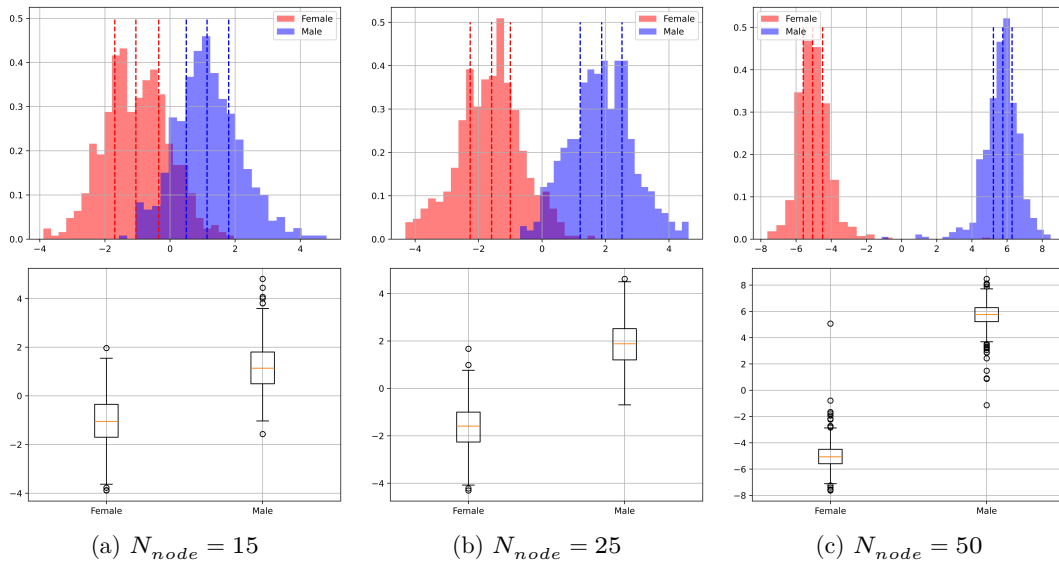


Figure 4: LDA for sFC.

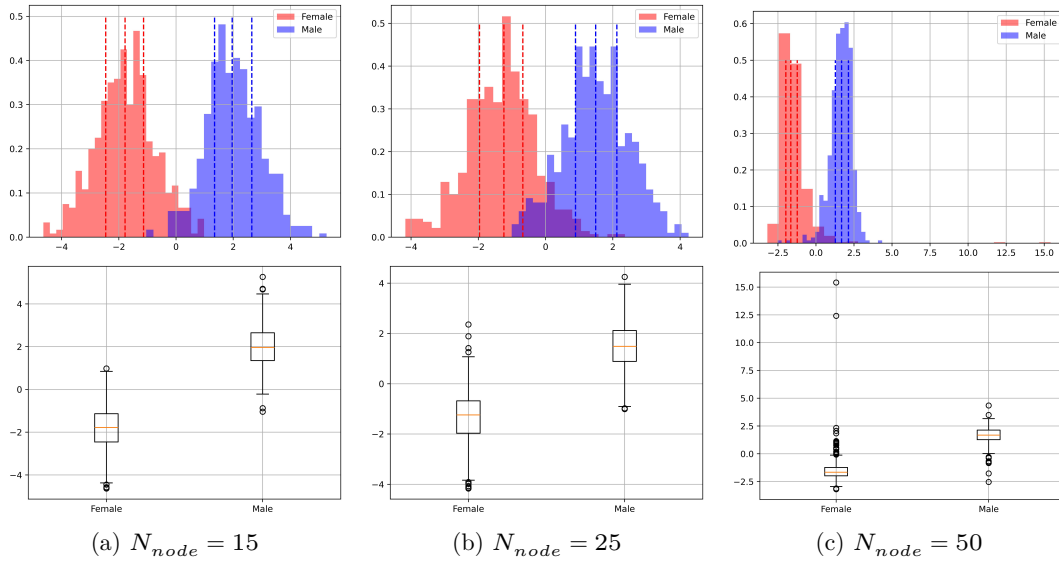


Figure 5: LDA for dFC.

3.2 Neuroscientific interpretations

The most significant portion of nodes was calculated based on the direction vectors obtained from fitting the LDA model to identify brain regions with significant sex differences. For static brain networks, the direction vectors were used directly; for dynamic brain networks, the mean of all direction vectors was used. The results were sorted by mode size and the brain connections corresponding to the top 10% largest elements were taken, and then the intersection of the results obtained for static and dynamic brain networks with the same number of nodes was taken.

4 Discussion

In our experiments, we use CNN and SVM to process brain network data, and record the accuracy rates and AUC from these 2 models respectively. When comparing the same metrics under different models (such as the AUC from 2 models), we find that CNN gets higher AUC than SVM, while they have similar performances on the accuracy rate. This might be attributed to feature redundancy from data processed by CNN, which means convergence from features extracted by different convolutional kernels.

One possible solution for this issue is to set the coefficients of CNN to be orthogonal. On the one hand, it might ensure the unique information captured by different convolutional kernels and reduce the correlation among features, which improves the efficiency of feature extraction. On the other hand, by maintaining the orthogonality of the weight matrix, orthogonal initialization could alleviate the explosion and vanishing of gradients [1], which accelerating the convergence rate of models and increasing the efficiency and performance of training.

Additionally, when pre-processing time series data, choosing a reasonable size and moving step for sliding window might lead to more precise brain functional connectivity data for us. Such adjustment could improve both time and frequency resolution and the capture efficiency of signal characteristics and overall trends [2]. To achieve this, we could use Fourier analysis [3] or wavelet analysis [4] to enhance our experiments. These 2 methods could help us to analyse complex patterns from functional connectivity data. To be more specific, the former is to decompose the periodic signal and the latter is to provide the local features of the signal in the time and frequency domains [5].

Finally, we use linear classifier in our experiments and find that both dynamic and static functional connectivity data are linearly separable. But this might not work well if the underlying relationships between the classes are non-linear or if the data contains complex interactions that cannot be captured by a linear model. In this condition, we might consider to use non-linear classifier such as quadratic ones to partition data, since the quadratic could consider the inequality of the in-class covariance matrix, the decision boundary is allowed to take a quadratic form [6], so as to better adapt to the complex structure in the data.

References

- [1] El Mehdi Achour, François Malgouyres, and Franck Mamalet. Existence, stability and scalability of orthogonal convolutional neural networks. *arXiv [math.ST]*, 2021.
- [2] Maxime Leiber, Yosra Marnissi, Axel Barrau, and Mohammed El Badaoui. Differentiable short-time fourier transform with respect to the hop length. 2023.
- [3] D Mantini, M G Perrucci, C Del Gratta, G L Romani, and M Corbetta. Electrophysiological signatures of resting state networks in the human brain. *Proc. Natl. Acad. Sci. U. S. A.*, 104(32):13170–13175, 2007.
- [4] Alessio Medda, Lukas Hoffmann, Matthew Magnuson, Garth Thompson, Wen-Ju Pan, and Shella Keilholz. Wavelet-based clustering of resting state MRI data in the rat. *Magn. Reson. Imaging*, 34(1):35–43, 2016.
- [5] Tiantian Guo, Tongpo Zhang, Enggee Lim, Miguel Lopez-Benitez, Fei Ma, and Limin Yu. A review of wavelet analysis and its applications: Challenges and opportunities. *IEEE Access*, 10:58869–58903, 2022.
- [6] Javier Rasero, Hannelore Aerts, Marlis Ontivero Ortega, Jesus M Cortes, Sebastiano Stramaglia, and Daniele Marinazzo. Predicting functional networks from region connectivity profiles in task-based versus resting-state fMRI data. *PLoS One*, 13(11):e0207385, 2018.
- [7] Matthew Leming and John Suckling. Deep learning for sex classification in resting-state and task functional brain networks from the UK biobank. *Neuroimage*, 241(118409):118409, 2021.

A Supplementary Material

A.1 Ablation study for SVM model

Method	Node	Data	min ACC/AUC	mean ACC/AUC	max ACC/AUC
LinearSVM	15	sFC	0.7363/0.7369	0.8083/0.8078	0.8706/0.8756
LinearSVM	25	sFC	0.8060/0.8059	0.8714/0.8708	0.9204/0.9202
LinearSVM	50	sFC	0.8905/0.8905	0.9357/0.9357	0.9751/0.9749
LinearSVM	15	dFC	0.6866/0.6919	0.7746/0.7733	0.8507/0.8534
LinearSVM	25	dFC	0.7861/0.7874	0.8739/0.8730	0.9204/0.9206
LinearSVM	50	dFC	0.8806/0.8813	0.9295/0.9300	0.9652/0.9666
Nu-SVM	15	sFC	0.7562/0.7571	0.8221/0.8219	0.8856/0.8847
Nu-SVM	25	sFC	0.8259/0.8257	0.8791/0.8782	0.9303/0.9302
Nu-SVM	50	sFC	0.8458/0.8458	0.9191/0.9194	0.9602/0.9608
Nu-SVM	15	dFC	0.7313/0.7324	0.8066/0.8056	0.8706/0.8674
Nu-SVM	25	dFC	0.8109/0.8121	0.8811/0.8802	0.9303/0.9296
Nu-SVM	50	dFC	0.8308/0.8300	0.9021/0.9022	0.9552/0.9579

Table 4: Ablation study for SVM.

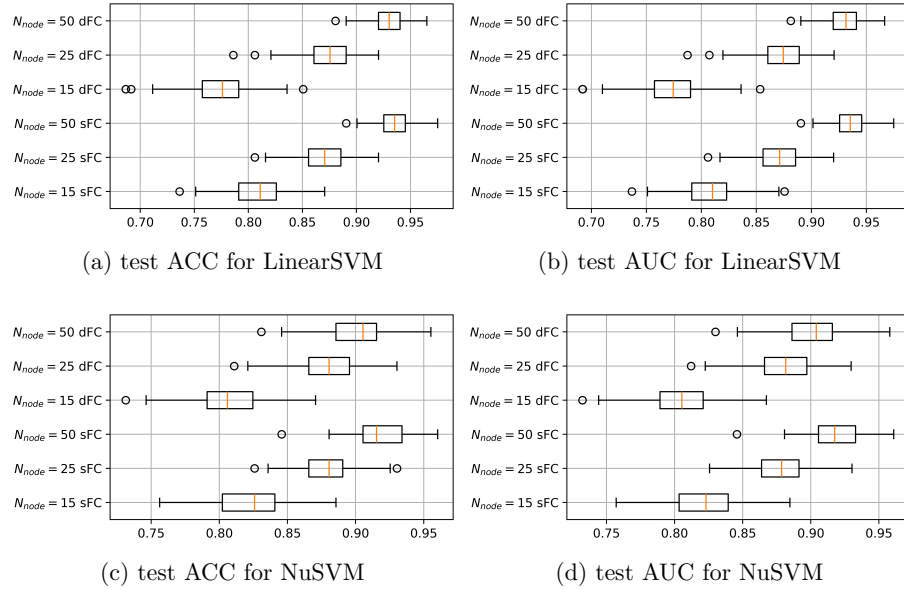


Figure 6: Results of SVM.

A.2 Ablation study for CNN model

Data	Dropout	Channel	min ACC/AUC	mean ACC/AUC	max ACC/AUC
sFC	0.0	1	0.5224/0.8108	0.7957/0.8855	0.8706/0.9307
sFC	0.0	2	0.7164/0.8273	0.8001/0.8876	0.8756/0.9281
sFC	0.0	4	0.7363/0.8189	0.7988/0.8863	0.8607/0.9337
sFC	0.1	1	0.5174/0.8041	0.7952/0.8870	0.8756/0.9355
sFC	0.1	2	0.7164/0.8318	0.7986/0.8885	0.8756/0.9294
sFC	0.1	4	0.7313/0.8276	0.8038/0.8911	0.8607/0.9317
dFC	0.0	1	0.5871/0.7160	0.7737/0.8670	0.8557/0.9216
dFC	0.0	2	0.6915/0.7824	0.7811/0.8630	0.8507/0.9209
dFC	0.0	4	0.7015/0.8028	0.7787/0.8584	0.8408/0.9148
dFC	0.1	1	0.5522/0.7140	0.7735/0.8656	0.8458/0.9209
dFC	0.1	2	0.6617/0.7942	0.7771/0.8692	0.8408/0.9110
dFC	0.1	4	0.7164/0.7987	0.7813/0.8666	0.8408/0.9171

Table 5: Ablation study for $N_{\text{node}} = 15$.

Data	Dropout	Channel	min ACC/AUC	mean ACC/AUC	max ACC/AUC
sFC	0.0	1	0.5075/0.7475	0.8462/0.9265	0.9104/0.9634
sFC	0.0	2	0.7662/0.8731	0.8470/0.9225	0.9104/0.9599
sFC	0.0	4	0.7512/0.8650	0.8468/0.9220	0.9055/0.9603
sFC	0.1	1	0.5124/0.7431	0.8547/0.9356	0.9154/0.9688
sFC	0.1	2	0.7711/0.8598	0.8581/0.9358	0.9254/0.9728
sFC	0.1	4	0.7711/0.8730	0.8562/0.9339	0.9104/0.9638
dFC	0.0	1	0.6269/0.7168	0.8450/0.9338	0.9303/0.9788
dFC	0.0	2	0.7463/0.8662	0.8594/0.9416	0.9254/0.9787
dFC	0.0	4	0.7960/0.9130	0.8672/0.9437	0.9154/0.9783
dFC	0.1	1	0.5771/0.6996	0.8391/0.9319	0.9254/0.9753
dFC	0.1	2	0.7612/0.8584	0.8618/0.9441	0.9204/0.9752
dFC	0.1	4	0.7264/0.8902	0.8606/0.9426	0.9104/0.9739

Table 6: Ablation study for $N_{\text{node}} = 25$.

Data	Dropout	Channel	min ACC/AUC	mean ACC/AUC	max ACC/AUC
sFC	0.0	1	0.5572/0.7721	0.9015/0.9689	0.9602/0.9947
sFC	0.0	2	0.7512/0.8462	0.9218/0.9762	0.9701/0.9941
sFC	0.0	4	0.8856/0.9589	0.9248/0.9779	0.9602/0.9938
sFC	0.1	1	0.5124/0.7691	0.8960/0.9684	0.9652/0.9952
sFC	0.1	2	0.7363/0.8335	0.9147/0.9746	0.9652/0.9947
sFC	0.1	4	0.8358/0.9562	0.9178/0.9778	0.9652/0.9940
dFC	0.0	1	0.6766/0.8767	0.8799/0.9689	0.9552/0.9924
dFC	0.0	2	0.7711/0.9366	0.9041/0.9733	0.9552/0.9917
dFC	0.0	4	0.8507/0.9543	0.9122/0.9766	0.9602/0.9946
dFC	0.1	1	0.7363/0.8511	0.8945/0.9714	0.9602/0.9940
dFC	0.1	2	0.8109/0.8966	0.9027/0.9716	0.9552/0.9925
dFC	0.1	4	0.7711/0.9128	0.9040/0.9713	0.9552/0.9930

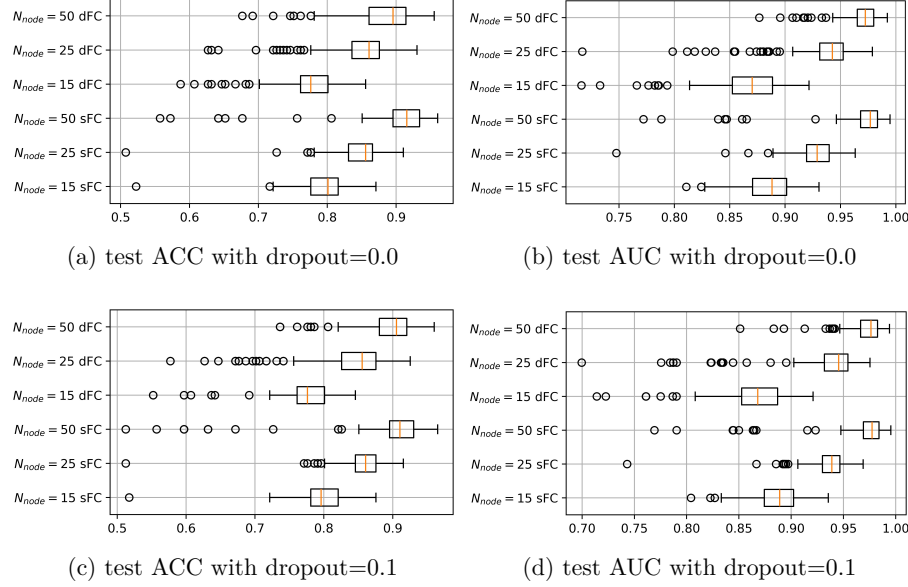
Table 7: Ablation study for $N_{node} = 50$.

Figure 7: Results of CNN model with channel = 1.

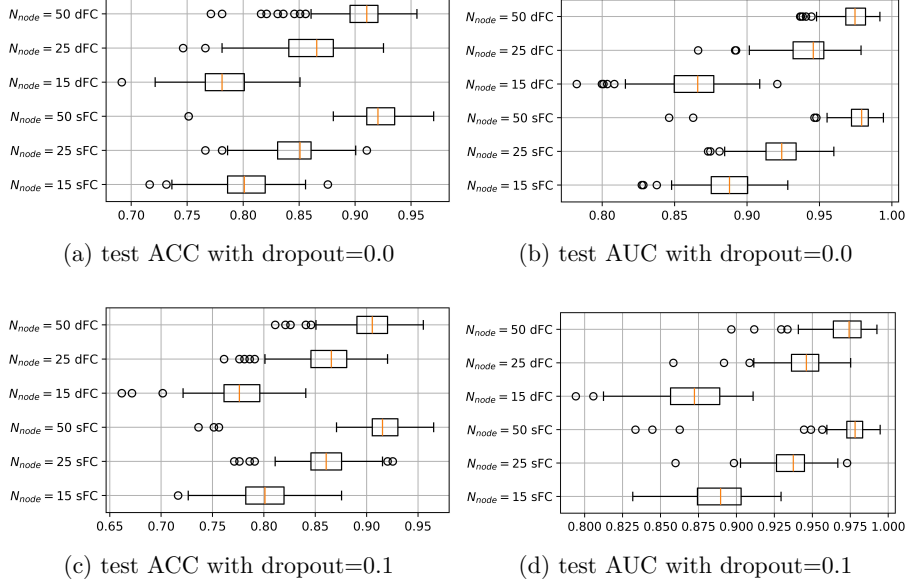


Figure 8: Results of CNN model with channel = 2.

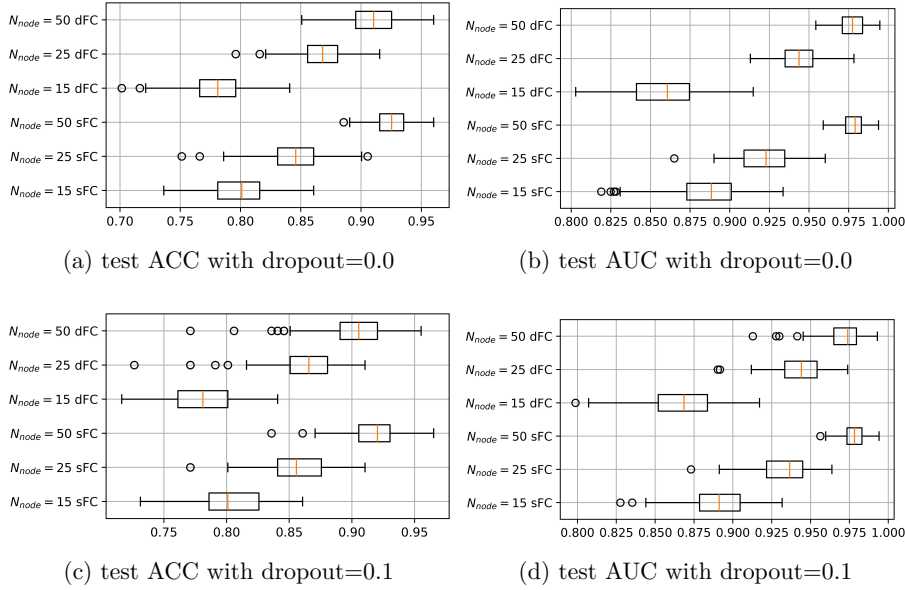


Figure 9: Results of CNN model with channel = 4.

A.3 Analysis for repetitions

There are multiple choice for repetition times, e.g., in some article, this number is set to 300 [7]. Thus it is necessary to analysis how this parameter affect the result.

Assume that the results (AUC or ACC) $\{X_i\}_{i=1}^n$ for different test are independent and identically distributed (i.i.d.) with mean value μ and variance σ^2 , then from central limit theorem

$$Y_n = \frac{\sum_{i=1}^n X_i - n\mu}{\sqrt{n}\sigma} \xrightarrow{D} N(0, 1).$$

Thus for all $\varepsilon > 0$,

$$P\left(|\bar{X}_i - \mu| \leq \frac{\sigma\varepsilon}{\sqrt{n}}\right) = P(|Y_n - E(Y_n)| \leq \varepsilon) = \Phi(\varepsilon) - \Phi(-\varepsilon),$$

where $\Phi(x)$ is the cumulative distribution function of the standard normal distribution.

We compute the variance of samples $\sigma \leq \sqrt{0.007} \leq 0.1$, which implies that if choose $\varepsilon = \sqrt{n}/\delta$, then

$$P\left(|(\bar{X}_i - \mu)| \leq \frac{0.1}{\delta}\right) \geq P\left(|\bar{X}_i - \mu| \leq \frac{\sigma}{\delta}\right) = \Phi\left(\frac{\sqrt{n}}{\delta}\right) - \Phi\left(-\frac{\sqrt{n}}{\delta}\right).$$

Then for $n = 150$, the result is shown as Table 8, which implies that the results can reaches an error lower than 1%.

$\delta = 5$	$P(\bar{X}_i - \mu \leq 0.02) \geq 0.9857$
$\delta = 8$	$P(\bar{X}_i - \mu \leq 0.0125) \geq 0.8742$
$\delta = 10$	$P(\bar{X}_i - \mu \leq 0.01) \geq 0.7793$
$\delta = 12.5$	$P(\bar{X}_i - \mu \leq 0.008) \geq 0.6728$
$\delta = 16$	$P(\bar{X}_i - \mu \leq 0.00625) \geq 0.5560$
$\delta = 20$	$P(\bar{X}_i - \mu \leq 0.005) \geq 0.4597$

Table 8: Probability of errors.